RSC Advances

ROYAL SOCIETY OF CHEMISTRY

www.rsc.org/advances

An efficient Ag-Nanoparticle embedded semi-IPN hydrogel for catalytic Applications

Manjusha V. Patwadkar[1], Chinnakonda S. Gopinath[2,3], Manohar V. Badiger[1,3]*

[1] Polymer Science and Engineering Division
CSIR-National Chemical Laboratory
Dr. Homi Bhabha Road, Pune 411 008, India

[2] Catalysis Division,
CSIR-National Chemical Laboratory,
Dr. Homi Bhabha Road, Pune-411008, India

[3]Center of Excellence on Surface Science,
CSIR-National Chemical Laboratory,
Dr. Homi Bhabha Road, Pune-411 008, India

*E-mail: mv.badiger@ncl.res.in

Abstract

Silver nanoparticle embedded Semi-IPN hydrogels based on combination of Poly(acrylamide) and Poly(aspartic acid) were synthesized .These Semi-IPN hydrogel networks can potentially serve as micro-or nano reactors for entrapment of metal nanoparticles. Current methodology allows us to entrap metal nanoparticles throughout hydrogel networks via poly(aspartic acid) chains which are dispersed homogeneously in the gel matrix. The Ag-NPs were characterized by UV–vis absorption spectroscopy, Transmission electronic microscopy (TEM), X-ray diffraction (XRD) and Energy dispersive X-ray analysis (EDAX). The Ag embedded hydrogels catalyze the reduction of 4-nitrophenol to 4-aminophenol in the presence of $NaBH_4$ very efficiently at room temperature with good recyclability upto 3 cycles.

Introduction

Metal nanoparticles exhibit number of specific properties that are markedly different from their bulk metal properties.[1] Therefore, show potential applications in catalytic, controlled release technology, electronics, photonics and sensor fields.[2-8] Particularly, metal nanoparticles are found to be very efficient catalyst systems for large number of chemical reactions owing to their

property of large surface area to volume ratio. For example, Witham etal. have reported on the design and synthesis of novel electrophilic platinum nanoparticles for homogenous catalytic reactions.[9] Olefinic hydrogenation and CO oxidation at low temperature by Au-NPs [10-12] and hydrosilylation reactions of olefins by Pd nanoparticles have been demonstrated.[13]A comprehensive review covering different methods of synthesis of metal nanoparticles and their catalytic applications is reported in the literature.[14] However, metallic nanoparticles have a tendency to aggregate and loose their important properties. Hence, metallic nanoparticles need to be stabilized in solution to suit end applications.

In order to overcome the problem of aggregation in metal nanoparticles, many protective systems have been used to enhance the stability and dispersibility of these nanoparticles. For example, polysaccharides, polymeric latex particles,[15] micelles,[16-17] dendrimers[18], hydrogels[19-20] have been used to stabilize metal nanoparticles. Amongst these, hydrogels are attracting increasing attention lately and are used as carrier systems for the in-situ synthesis of metal nanoparticles.[21] The hydrophilic nature of hydrogels along with the 3-D network structure, results swelling in aqueous fluids containing metal salts and allows easy diffusion of metal ions through gel matrix. The polymer gel matrix with charge facilitates the immobilization of metal ions and upon reduction with reducing agent yields metal nanoparticles. The 3-D network structure of the hydrogels can be controlled and hence they can potentially serve as micro-or nano reactors for entrapment of metal nanoparticles. Further, the size and morphology of nanoparticles can be easily controlled by varying the composition of gel during the gelation process.

Although there are a few reports on the synthesis of metal nanoparticles in the polymeric gel matrix, the influence of hydrogel properties such as hydrophilicity, degree of swelling on the nanoparticle synthesis and the mechanical strength of the nanoparticles embedded hydrogels have not been investigated fully.

In this paper, we report on the design and synthesis of Ag-NPs embedded semi-IPN hydrogel based on the combination of poly(acrylamide) and poly(aspartic acid). The presence of poly (aspartic acid) induces changes in the gel and facilitates the diffusion of more Ag^+ ions into the hydrogel through electrostatic interaction between $-COO^-$ groups of poly(aspartic acid) and Ag^+ ions. The Ag-NPs embedded hydrogel was characterized by UV-vis, X-ray photoelectron spectroscopy (XPS), X-ray diffraction (XRD) and Transmission electron microscopy (TEM).

The catalytic application of Ag-NPs embedded hydrogel was demonstrated using a model reduction reaction of 4-nitrophenol to 4-aminophenol.

Experimental

Acrylamide (AM), N,N′-Methylenebisacrylamide (MBA) , N,N,N′,N′-Tetramethylethylenediamine (TEMED), ammonium persulfate (APS) were purchased from Aldrich (USA) and used as received. Sodium salt of Poly(aspartic acid) [PAS] with an average molecular weight of 64 KDa was synthesized in our laboratory by polycondensation of L-aspartic acid reported earlier.[22] Silver nitrate ($AgNO_3$) was procured from S. D. Fine Chemicals Ltd (India) and sodium borohydride ($NaBH_4$) was purchased from Merck (India).

Synthesis of Semi-IPN hydrogel

Poly(acrylamide) (PAm) / Poly(aspartic acid) (PAS) Semi-IPN hydrogels were synthesized by free radical polymerization of acrylamide (Am) monomer in the presence of PAS polymer under nitrogen atmosphere. N, N'- methylenebisacrylamide (MBA) was used as a crosslinker and ammonium persulfate (APS) and tetramethylethylenediamine (TEMED) were used as initiator and accelerator for the reaction respectively. In a typical reaction, known amount of acrylamide monomer and PAS were dissolved in distilled water. To the reaction mixture, MBA was added and dissolved completely. Upon complete dissolution, APS and TEMED were added and the polymerization was carried out at 30°C under N_2 atmosphere. The gelation took place in 10 minutes and polymerization was further carried out for 24 hours to complete the reaction. The obtained hydrogels were immersed in water to remove any unreacted monomers. Finally, hydrogels were sliced into discs of different diameter and thickness and dried to obtained xerogels. Semi-IPN hydrogels with different contents of PAS were prepared and their feed compositions are given in Table 1.

Table 1: Feed composition for the synthesis of semi-IPN Hydrogels

Sr.No.	Samples (wt. ratio)	Am (g)	PAS (g)	MBA (g)	APS (g)	TEMED (µl)
1	PAm	1.0	0.0	0.027	0.01	10
2	PAm/PAS 80/20	1.0	0.25	0.027	0.01	10
3	PAm/PAS 60/40	1.0	0.66	0.027	0.01	10
4	PAm/PAS 50/50	1.0	1.0	0.027	0.01	10

Preparation of Ag-NPs embedded Semi-IPN hydrogel

Discs, equilibrium swollen in water were immersed in a beaker containing 50 ml of 5mM $AgNO_3$ aqueous solution and allowed to equilibrate for 1 day. In this step, the silver ions diffuse into the gel network. Then, silver ion soaked gels (colorless) were immersed in 50 ml of 10mM $NaBH_4$ reducing agent and kept for 3 hrs. Upon reduction of silver ions to silver nanoparticles, the gels became dark brown in color which is an indication of the formation of Ag-NPs. The obtained hydrogels were denoted as Ag-NPs embedded Semi-IPN hydrogels.

Characterization

UV-visible spectra of Ag-NPs embedded semi-IPN hydrogels were recorded using UV-1601-PC SHIMADZU UV- spectrophotometer. X-ray diffraction measurements were performed on the Ag-NPs embedded Semi-IPN hydrogel using a Philips X'pert pro powder X-ray diffractometer operating with CuKα radiation (λ=0.15406 nm, Ni filter) generated at 40 kV and 30 mA X-ray diffractometer. The size of the Ag-NPs in hydrogels was determined using TEM FEI, TECNAI G2 F30 instrument operated at an accelerated voltage of 300 kV.

Swelling and Kinetics of Swelling

Fully dried Ag-NPs embedded Semi-IPN gels were accurately weighed and equilibrated in distilled water at 30°C for 3 days. The equilibrium Swelling ratio (Q) of the hydrogel was calculated using the following equation 1.

$$Q = \frac{W_s - W_d}{W_d} \times 100 - - - - - - - (1)$$

Where, W_s = mass of the equilibrium Swollen hydrogel

W_d = mass of xerogel

Further, the kinetics of Swelling was studied by measuring swelling of gels at different time intervals. The fractional uptake of water, 'F' at pre determined time, 't' was determined using equation of krosmeyer and Pepps[23]

$$F = \frac{W_t}{W_s} = Kt^n \quad ------- (2)$$

Where, W_t and W_s are mass of swollen gel at time't' and mass of equilibrium swollen gel respectively. K is constant and 'n' is the diffusion exponent which provides information on swelling kinetics.

Catalytic Activity

The catalytic activity of the Ag-NPs embedded Semi-IPN hydrogel was evaluated for reduction reaction of 4-nitrophenol (4-NP) to 4-aminophenol (4-AP) by $NaBH_4$ by monitoring the electronic absorption of reaction mixture as a function of time. In a typical experiment, 1.4 ml of water, 0.3 ml of 2 mM 4-NP was taken in a quartz cell and 1 ml of 0.03M $NaBH_4$ was added. To this reaction mixture, 10 mg of Ag-NPs embedded Semi-IPN gel was added. The progress of reaction was monitored by recording the time-dependent absorbance using UV-vis spectrophotometer in the scanning range of 200-800 nm at 30°C.

Reusability of the catalyst

After the first cycle of reaction, the Ag-NPs embedded Semi-IPN hydrogel was separated and washed 2-3 times with 50 ml distilled water. The washed hydrogel catalyst was subsequently taken for further cycles of reaction and evaluated using the above mentioned procedure.

Results and Discussion

Ag-NPs embedded Semi-IPN Hydrogel

Unprotected nanoparticles in general are unstable and hence coagulation or aggregation is unavoidable during the catalytic reactions.[24] Hydrogels with embedded metal nanoparticles combine the versatility of former with interesting catalytic properties of the later. In this work, we have synthesized Ag-NPs embedded semi-IPN hydrogel based on poly(acrylamide) (PAm) and poly(aspartic acid) (PAS). The hydrogel synthesis is performed in the presence of PAS, where in this PAS is physically entangled in the 3-D structure of PAm resulting into Semi-IPN hydrogel. The advantage with this combination of polymers is that, the PAm has an excellent hydrogel forming property with ease of formation of 3-D network structure. Whereas, PAS is a biocompatible, biodegradable, non-toxic polymer and has protecting and nucleating nature for metal nanoparticles. The gelation takes place at room temperature. Furthermore, PAS has ionizable -COOH groups which helps in absorbing more silver ions through electrostatic interactions between COO^- and Ag^+ ions. The Semi-IPN hydrogels swollen in aqueous $AgNO_3$ solution were subjected to reduction reaction in the presence of $NaBH_4$ to form Ag-NPs embedded Semi-IPN hydrogels. The schematic representation of the formation of Ag-NPs in Semi-IPN hydrogel is shown in figure 1.

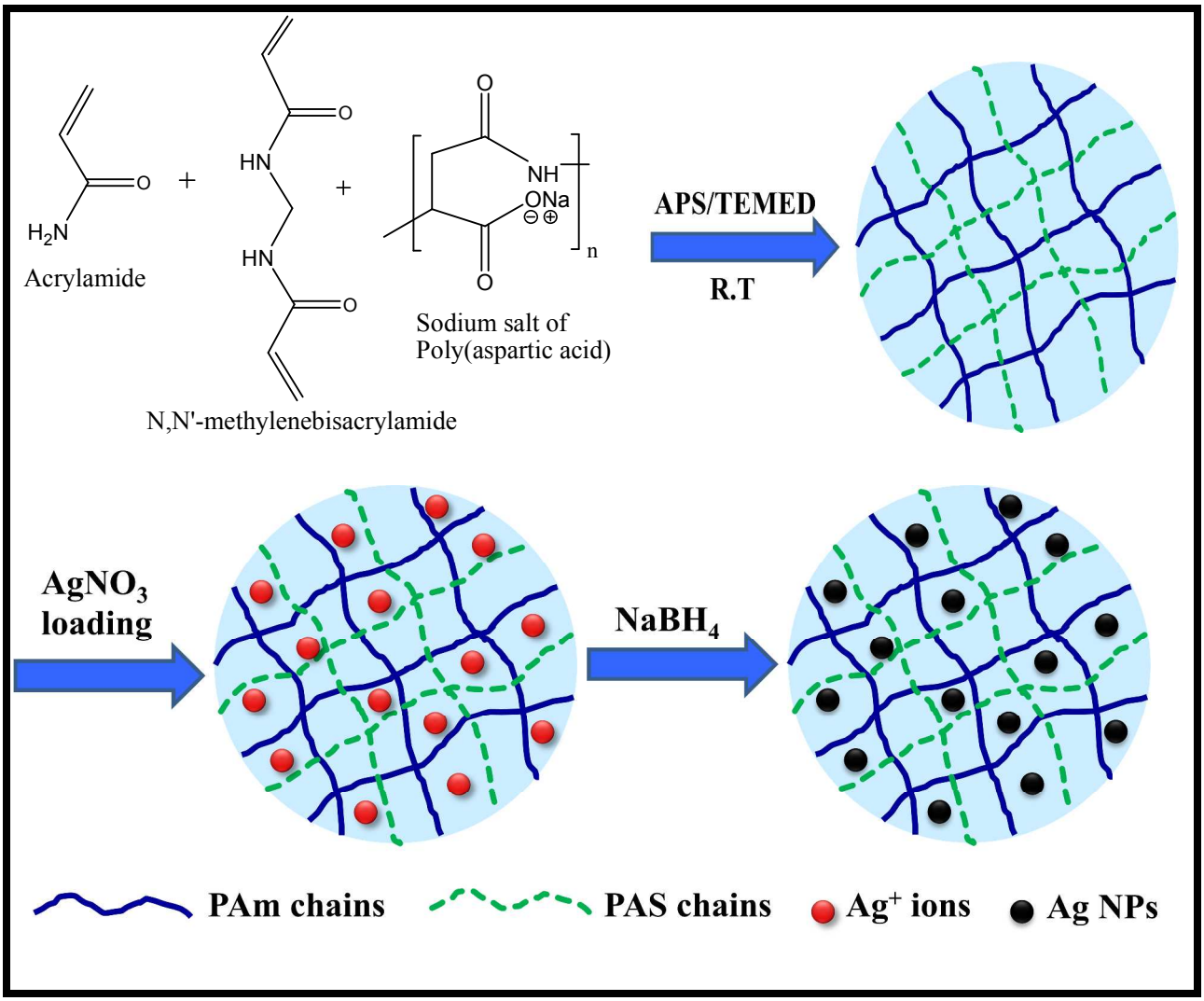

Figure 1: Schematic representation of formation of Ag-NPs in semi-IPN hydrogel

Swelling Studies

Figure 2(a) shows the influence of PAS content on the equilibrium swelling ratios (Q) of Semi-IPN hydrogels. It can be readily seen that, with same degree of crosslinking, PAm hydrogel without any PAS swells the least because of its non-ionic nature. However, as the PAS content increases, the Q value increases significantly. This could be attributed to the fact that, PAS contains ionizable -COOH groups and the Semi-IPN hydrogel become more ionic in nature and increases the hydrophilicity of the hydrogel. This results in enhancing the swelling ratios of hydrogels.

Figure 2(b) shows the swelling kinetics of Semi-IPN hydrogels. The *n* values of all ratios (100:0,80:20,60:40, 50;50) of PAm:PAS Semi-IPN hydrogels were calculated from the slopes of lines of log(F) against log(t) and found to be 0.625,0.664,0.734,0.839 respectively. This clearly indicated the transport in all the Semi- IPN hydrogels is Non-Fickian and dominated by diffusion.

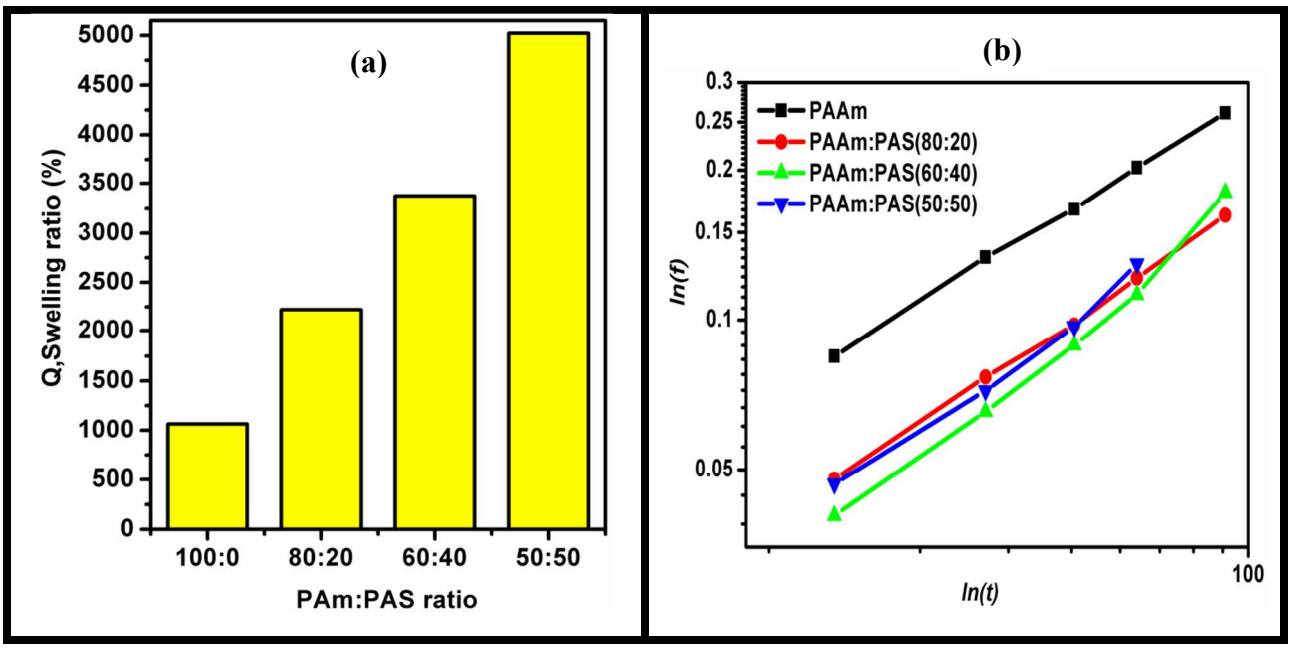

Figure 2: (a) Equilibrium swelling ratio (Q) of Semi-IPN hydrogels in water (b) Plot of ln(F) Vs ln(t)

In order to check the influence of pH on the swelling ratios of Semi-IPN hydrogels, the swelling ratios were determined in different pH solutions and the results are shown in figure 3. It is observed that the equilibrium swelling ratio is maximum in the pH range of 6-10 and exhibits lower values in the acidic pH range due to the unionized carboxylic groups of PAS. With increase in pH; the ionization of -COOH groups in PAS occurs and the electrostatic repulsive forces between ionized -COO^- groups in PAS leads to increased swelling ratios. However, at very high pH value, the electrostatic repulsive forces are screened and the swelling ratio decreases.

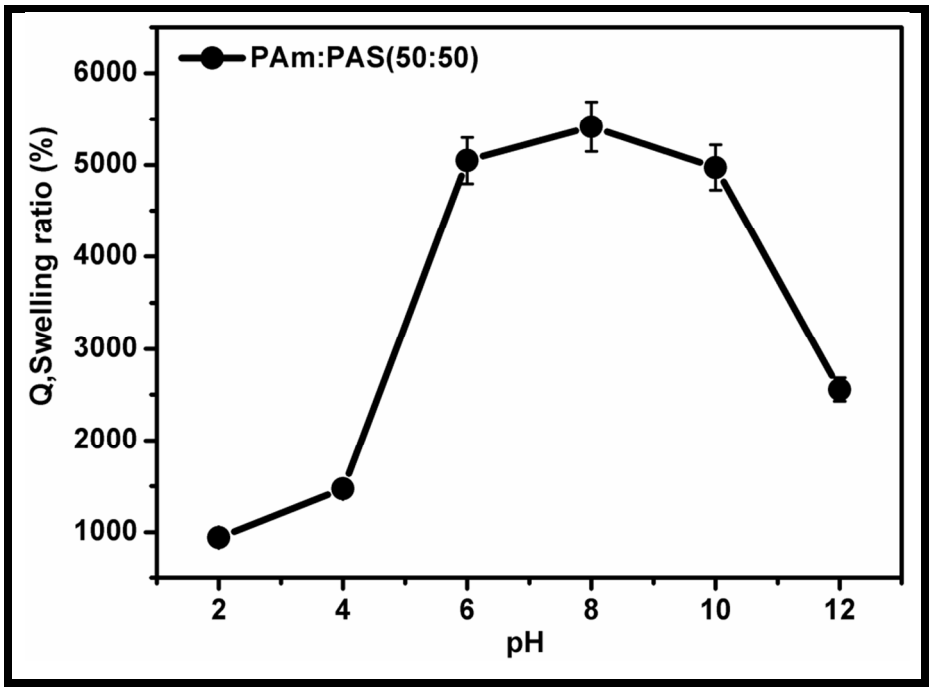

Figure 3: Equilibrium swelling ratio (Q) of PAm:PAS (50:50) sample in different pH solution

UV-vis spectroscopy

The presence of embedded Ag-NPs in the Semi-IPN hydrogel network was confirmed by UV-vis spectroscopy. The Semi-IPN hydrogels swollen in $AgNO_3$ solution were readily reduced using $NaBH_4$ which was indicated by the change in the colour of the hydrogel from colourless to dark brown. Figure 4 shows the distinct absorption peaks of Ag-NPs embedded Semi-IPN hydrogels at 410 nm due to the characteristics Surface Plasmon Resonance effect of Ag-NPs in the hydrogel.

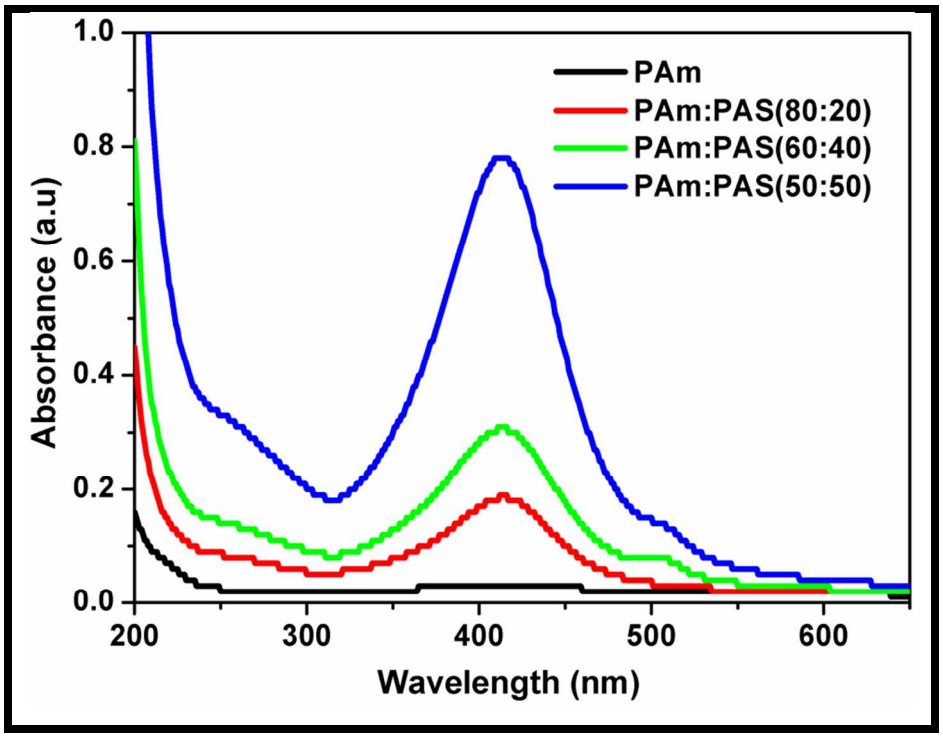

Figure 4: UV-vis spectra of Ag -NPs embedded Semi-IPN hydrogels

It was observed that with increase in PAS content in the hydrogel, the loading of silver salt in the hydrogel also increased which resulted in the formation of more Ag-NPs in the hydrogel. This is clearly seen in the intense absorption peaks of silver in the UV spectra of samples containing more PAS content. Further, the absence of peaks at 335 nm and 560 nm indicates that there is no aggregation of Ag-NPs in the hydrogel and the Ag-NPs are stable and well dispersed in the Semi-IPN hydrogel matrix[25]. This is confirmed by TEM which will be discussed in the later section.

X-ray diffraction

The crystalline nature of the Ag-NPs in the hydrogel was investigated by X-ray diffraction. The X-ray diffraction patterns of pure Semi-IPN hydrogel and Ag-NPs embedded hydrogel, are shown in figure 5. The diffractogram of Ag-NPs embedded hydrogel exhibits the presence of reflection peaks typical of a face centered cubic (fcc) structure of silver nanoparticles, with 2θ values of about 38.38° and 64.53° assigned to the lattice planes of face centered cubic (fcc) structure of Ag-NPs[26-27].

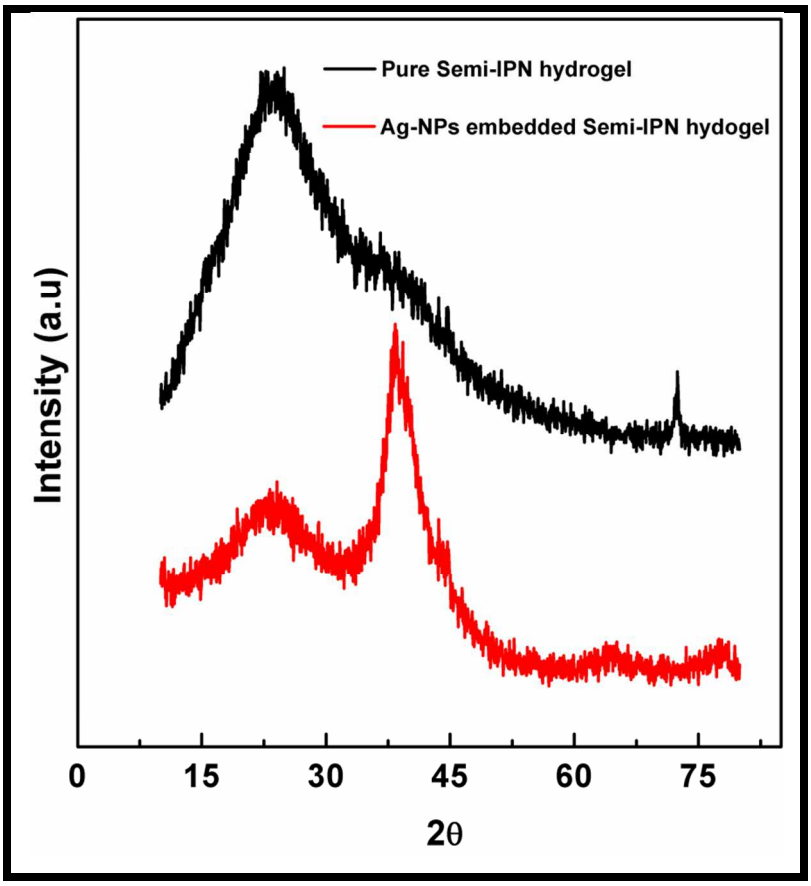

Figure 5: XRD patterns of pure Semi-IPN hydrogel and Ag-NPs embedded Semi-IPN hydrogel (50:50)

These peaks represent the crystalline nature of Ag-NPs embedded in the semi-IPN hydrogel matrix. Further, the absence of these peaks in the pure semi-IPN gel clearly indicates the amorphous nature of the hydrogel.

Transmission Electron microscopy (TEM)

To further confirm the formation of Ag-NPs and their morphology in the Semi-IPN hydrogel, the samples were analyzed using Transmission Electron Microscopy (TEM). We show in figure 6, the TEM images of Ag-NPs embedded PAm: PAS (50:50) and PAm hydrogel. It can be readily seen that, the Ag-NPs are uniformly dispersed in the hydrogel matrix with a size of 10-20 nm. The Ag-NPs are found to be spherical in shape and the selective area electron diffraction

(SAED) pattern of Ag-NPs is clearly observed as diffraction rings which is attributed to the face-centered cubic (fcc) structure of Ag-NPs.

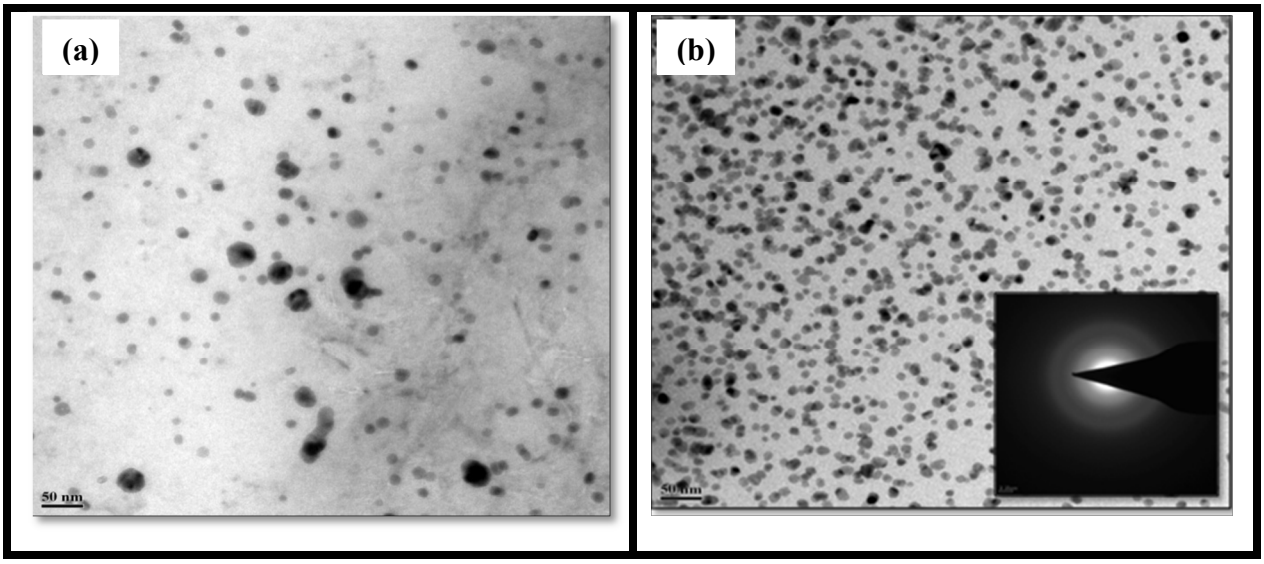

Figure 6: TEM images of Ag-NPs in (a) PAm and (b) PAm:PAS (50:50) hydrogel

The formation of Ag-NPs in the PAm gel can also be seen in the TEM micrograph of PAm hydrogel. However, the number of Ag-NPs formed in the PAm hydrogel is very small which could be due to the less absorption of silver salt in the PAm hydrogel. This observation is clearly supported by our UV-absorption study of Ag-NPs embedded PAm hydrogel, in which the intensity of absorption peak is very weak. However, with the incorporation of PAS into PAm hydrogel, more absorption of silver salt into hydrogel takes place resulting into more number of Ag-NPs. PAS helps in anchoring more Ag-NPs into the hydrogel matrix.

Energy dispersive X-ray analysis (EDAX)

To confirm the formation of Ag-NPs and % of Ag present in hydrogel, the samples were analyzed by energy dispersive X-ray analysis (EDAX). Metallic silver nanocrystals generally show typical optical absorption peak approximately at 3 keV due to Surface Plasmon Resonance. Figure 7(a) shows that in the case of PAm hydrogel, there is very less number of Ag-NPs formed which is insensitive to be detected by EDAX. However, in the case of PAm:PAS (50:50) (figure 7b) we could see a strong signal in the Ag region confirming the presence of Ag-NPs in the gel. We also show in Table-2, the composition of each element (wt %) present as determined by

EDAX measurement. The results clearly show that the amount of silver is more in semi-IPN hydrogel of PAm:PAS (50:50).

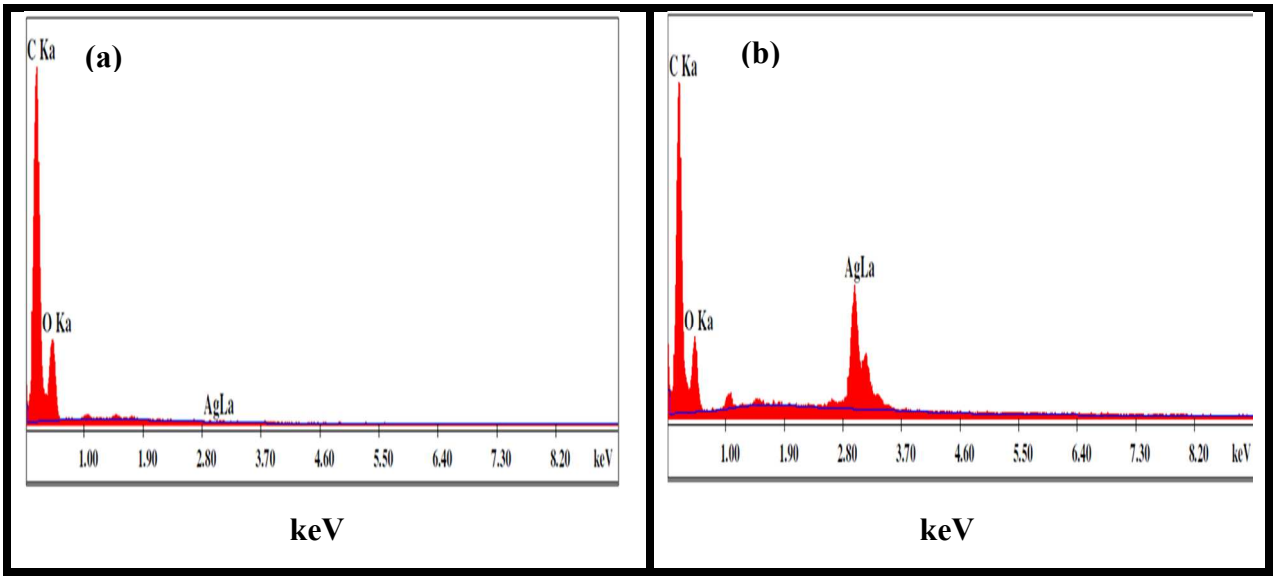

Figure 7: EDAX images of (a) Ag embedded PAm hydrogel and (b) Ag embedded PAm:PAS (50:50) hydrogel

Table 2: Weight % of each element by EDAX

Element	Ag embedded PAm Hydrogel (Wt %)	Ag embedded hydrogel PAm:PAS (50:50) (Wt %)
C (K)	73.83	61.61
O (K)	26.17	21.59
Ag (L)	0	16.79
Total	100.00	100.00

X-ray Photoelectron Spectroscopy (XPS)

To obtain further information on the Ag-NPs in the hydrogel matrix, we performed XPS measurements on the sample PAM:PAS (50:50) with Ag-NPs embedded into it. Ag 3d and C 1s core level spectra of Ag-NPs embedded gel are shown in figure 8.

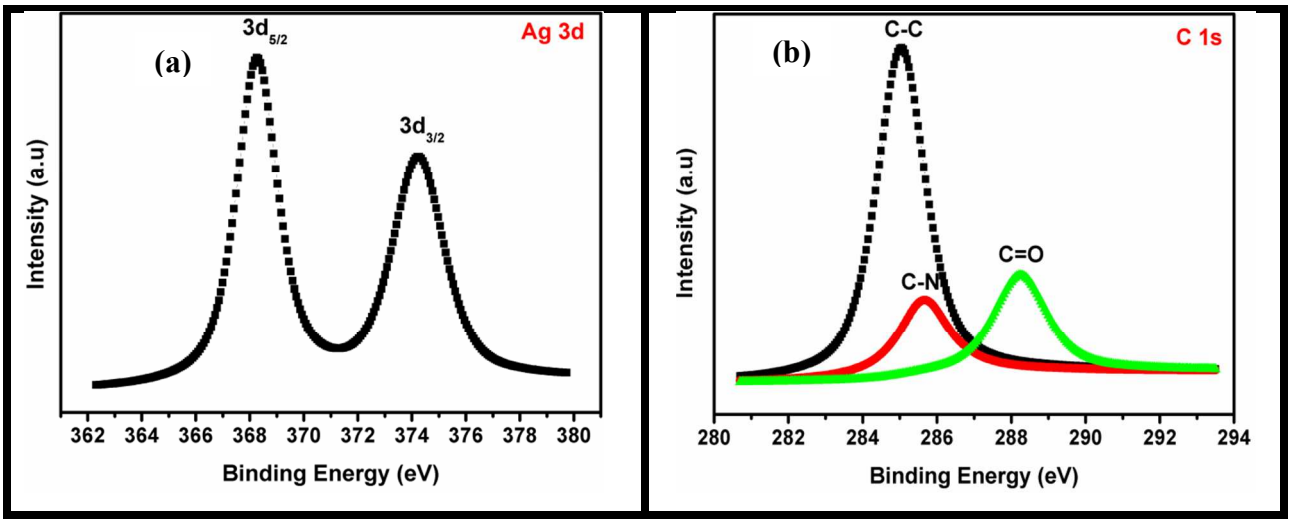

Figure 8: Core level XPS spectra of (a) Ag 3d (b) C 1s of PAm:PAS (50:50) hydrogel

Ag $3d_{5/2}$ and $3d_{3/2}$ spin-orbit coupled core levels are observed at 368 eV and 374 eV respectively. Ag $3d_{5/2}$ peak at 367.5± 0.2 eV corresponds to metallic Ag (Ag^0).This confirms the presence of Ag in metallic state.

C 1s core level spectra are shown in figure 8(b). It can be readily seen that peak at 285 eV in a typical feature of alkyl carbon. The peak at 285.6 eV corresponds to carbon attached to nitrogen (C-N) and the peak at 288.2 eV can be attributed to the carbonyl group .The above observations clearly indicate the presence of Ag-NPs in the gel matrix.

Catalytic activity of Ag-NPs embedded Semi-IPN hydrogel

The catalytic reduction of 4-NP to 4-AP was performed using Ag-NPs embedded Semi-IPN hydrogel. The reduction of 4-NP by sodium borohydride ($NaBH_4$) over a Ag catalyst is important for practical application. Silver has drawn great interest because of its high catalytic activity for various chemical reactions. The product 4-AP is an important chemical which has

wide range of application in analgesic and antipyretic drugs, photographic developers, corrosion inhibitors, and anticorrosion lubricants etc.[28]

Although the reduction of 4-NP to 4-AP using $NaBH_4$ is thermodynamically favorable, the reaction rate is very low and sluggish. However, in the presence of Ag-NPs, which acts as catalyst, the reaction proceeds very fast and the reaction time reduces significantly. The conversion of 4-NP to 4-AP occurs via an intermediate, 4-nitrophenolate ion formation. As shown in figure 9, 4-NP exhibits a strong absorption peak @ 317 nm, which shifts to 400 nm upon addition of $NaBH_4$ due to formation of 4-nitrophenolate ion in the alkaline medium. It is important to note that, although the shift has occurred, the absorption intensity has remained unchanged even after the 60 minutes, indicating that the reduction of 4-NP to 4-AP did not proceed in the absence of catalyst [See figure 9 (b)]. We also show that just by the addition of precursor semi-IPN hydrogel without Ag NPs to reaction medium did not reduce 4-NP to 4-AP [See figure 9 (c)].

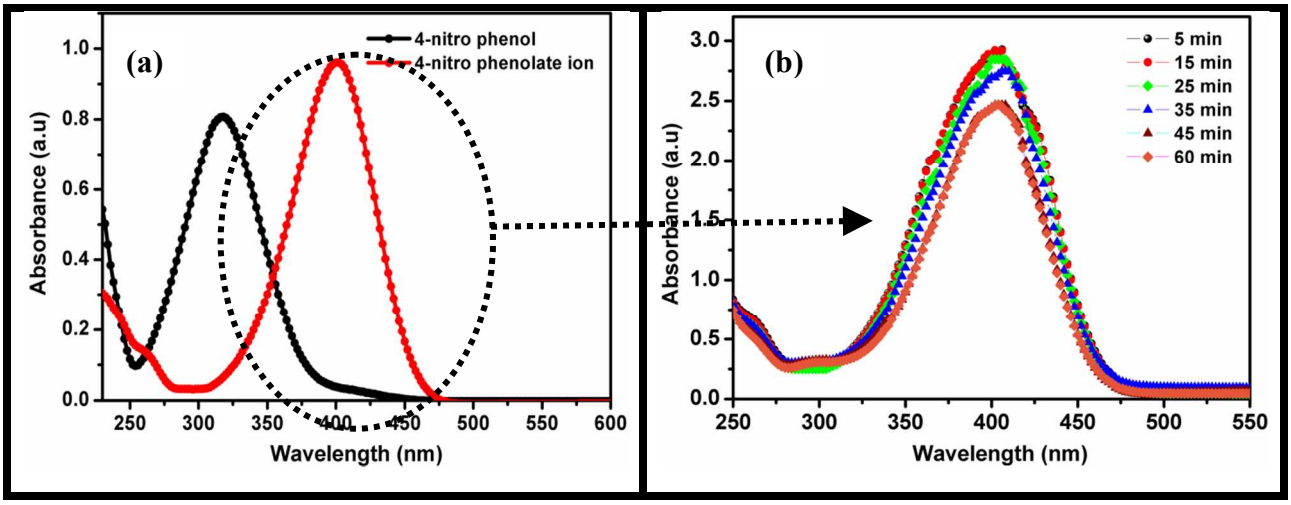

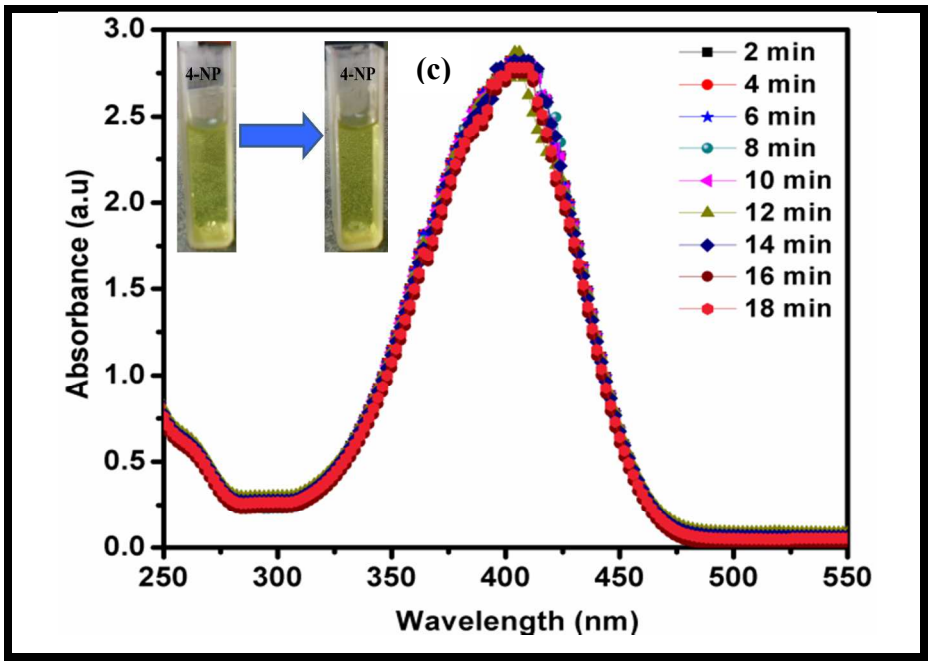

Figure 9: UV spectra of (a) 4-NP and 4-nitro phenolate ion (b) reduction of 4- NP using sodium borohydride without catalyst as a function of time (c) reduction reaction of 4-NP using only precursor Semi-IPN hydrogel without AgNPs

Upon addition of Ag-NPs embedded Semi-IP hydrogel to the reaction medium, there was a gradual decrease in the intensity of absorption peak at 400 nm with time and simultaneously, there was an appearance of new absorption peak at 298 nm indicating the reduction of 4-NP and the formation of 4-AP as shown in figure 10.

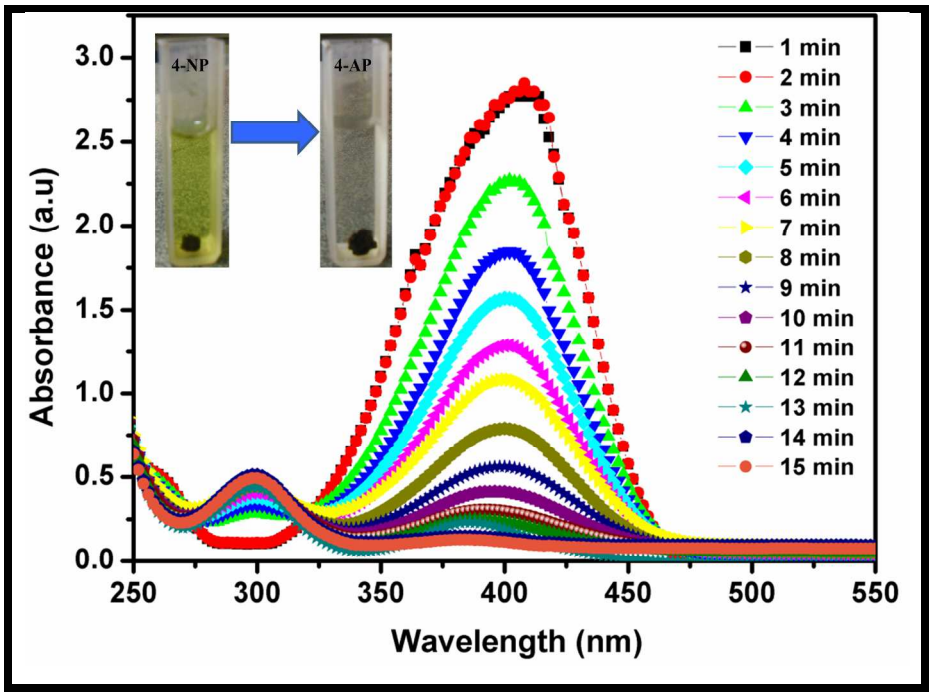

Figure 10: Catalytic effect of Ag embedded gel on reduction of 4-NP

The completion of reaction, which happened in ≈ 20 minutes, was indicated by the slow fading of yellow colour of the reaction mixture. In order to understand the kinetics of the reaction, the decrease in the concentration of reactant w.r.t time was measured. The kinetics of reaction could be described by equation,

$$\ln(C/C_0) = -Kt \ldots\ldots\ldots\ldots\ldots\ldots (3)$$

Where 'k' is the first order rate constant (since the concentration of $NaBH_4$ is in large excess) 't' is the reaction time, 'C' and 'C_0' are the concentration of 4-NP at time't' and '0' respectively.

Figure 11 shows the linear plot between ln (C/C_0) and reaction time't' for the reduction of 4-NP to 4-AP using Ag-NPs embedded semi-IPN hydrogel as catalyst. It can be readily seen from the figure that the reaction followed pseudo first order reaction kinetics with the rate constant determined from the slope of liner plot which was found to be 0.374 min^{-1}. The correlation coefficient of the linear plot was very good with the value =0.997

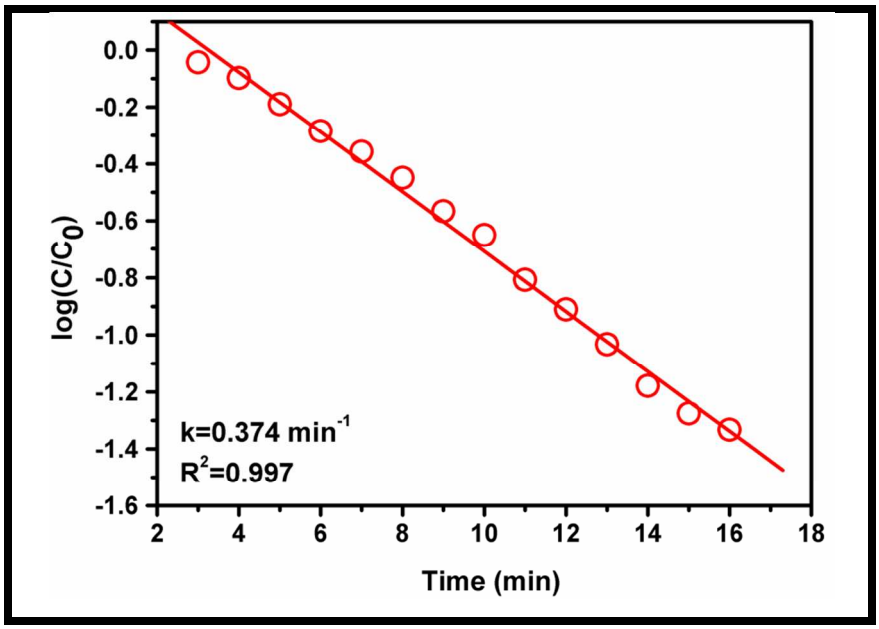

Figure 11: Plot of ln(C/C_0) against the reaction time for the reduction of 4-NP by $NaBH_4$ using catalyst

In order to study the effect of concentration of PAS on the catalytic activity, we performed the reduction of 4-NP to 4-AP using different ratios of PAm:PAS Ag-NPs embedded hydrogels. Figure 12 shows that, as the PAS content increases, the catalytic activity of hydrogel also increases. It reveals that 50:50 ratio has more number of Ag-NPs and also has more swelling ratio (Q) which increases rate of reaction as compared to PAm and 80:20 hydrogel. These results are again in agreement with our UV and TEM studies discussed in earlier sections.

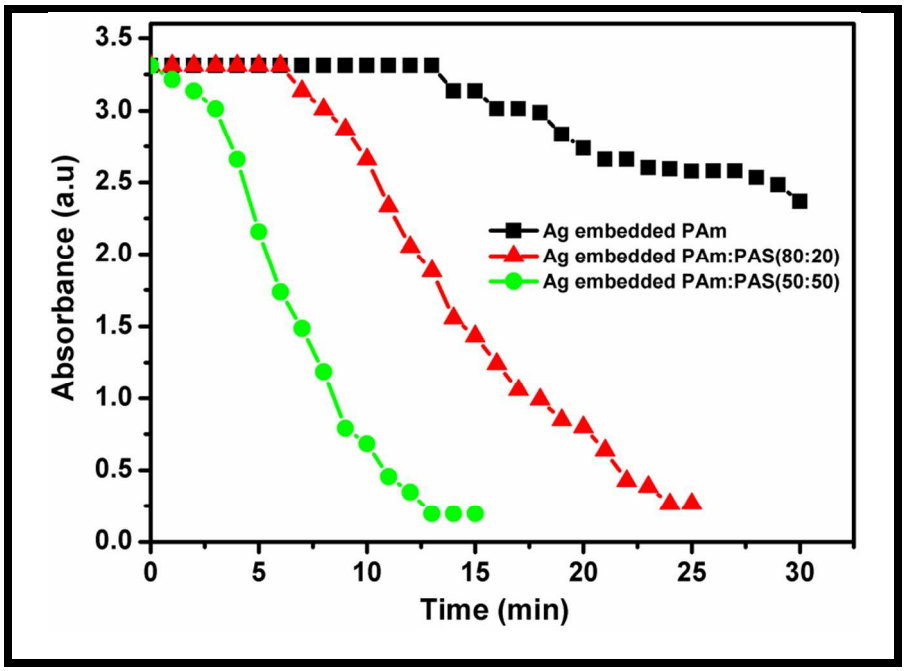

Figure 12: Catalytic effect of Ag-NPs embedded hydrogel with different ratio of PAm:PAS

Catalyst recycling

After completion of the first run of reaction, we also explored the repeated use of the same catalyst in successive multiple reaction runs. The Ag-NPs embedded Semi-IPN hydrogel could be easily separated from each cycle and washed with Milli Q water and dried under vacuum before taking it for the next reaction. We show in figure 13, the plots of C/C_0 versus reaction time for successive 3 cycles of reduction of 4-NP to 4-AP using the same reaction conditions. It can be readily seen that the Ag-NPs embedded Semi-IPN hydrogel can be successfully reused for 3 cycles without the loss of catalytic activity. However, there is slight decrease in the rate constants for successive cycles shown in figure 13(b) which may be attributed to the loss of Ag-NPs while washing in the intermittent stage. Never the less, these observations clearly indicate that the catalyst can be recycled for 3-4 cycles.

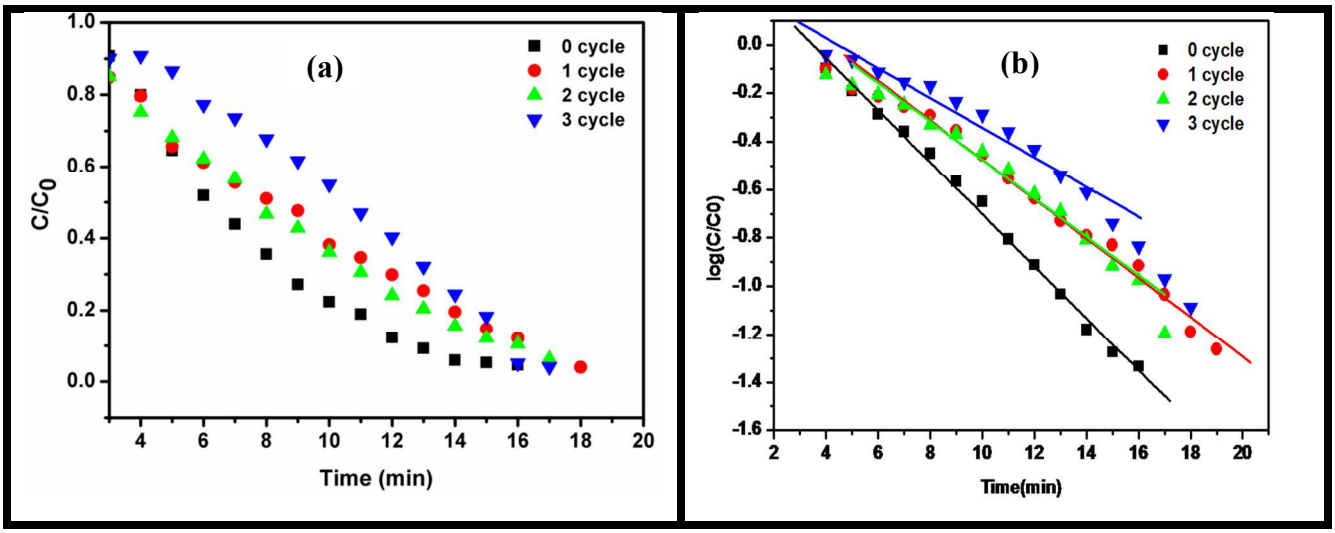

Figure 13: Plot of (a) C/C_0 and (b) log C/C_0 against the reaction time for successive three cycle reactions using catalyst

Conclusions

In summary, we have reported on the synthesis and characterization of Ag-NPs embedded hydrogel based on combination of poly(acrylamide) and poly(Aspartic acid). The formation of Ag-NPs confirmed by employing a variety of analytical methods, such as UV-Vis spectroscopy, which gave a surface Plasmon resonance in the range of 400-420 nm. The TEM images indicated the size of nanoparticles in the range of 10-20 nm. We also demonstrated the use of these Ag-NPs embedded hydrogel in the catalytic application for reduction of 4-NP to 4-AP. More importantly, the Ag-embedded hydrogel could be easily separated and reused for subsequent repeated cycles without losing the catalytic activity which is the most desired aspects.

Acknowledgements

MVP thanks CSIR, New Delhi for SRF

References:

1. Burda C, Chen X, Narayanan R, El-Sayed MA *Chem Rev*, 2005, 105, 1025-1102.
2. S. Xu, J. Zhang, C. Paquet, Y. Lin, E. Kumacheva, *Adv. Funct. Mater.* , 2003, 13, 468.
3. C.D. Jones, M.J. Serpe, L. Schroeder, L.A. Lyon, *J. Am. Chem. Soc*, 2004, 5292.
4. Liz-Marzan, *Langmuir*, 2006, 22, 32.
5. P. Liljeroth, D.Vanmaekelbergh, Ruiz, K. Kontturi, H. Jiang, E. Kauppinen, B.M. Quinn, *J. Am. Chem. Soc.* , 2004, 126, 7126.
6. P. V. Kamat, *J. Phys. Chem. B*, 2002, 106, 7729.
7. A. Biffis, B. Corain, *Adv. Mater.*, 2003, 15, 1551.
8. I. Willner, A.N. Shipway, *Chem. Commun*, 2001, 2035.
9. Cole A. Witham, Chia-Kuang Tsung, John N. Kuhn, Gabor A. Somorjai , *Nature Chemistry*, 2010, 2, 36-41.
10. G. J. Hutchings, *J.Material Chemistry* 2009, 19, 1222-1235.
11. Haruta M, Kobayashi T, Sano H, Yamada, *Chem.Lett* 1987, 405-407.
12. M. Haruta, *Chem. Res*, 2003, 3, 75-87.
13. Nathan Lewis, Larry N. Lewis, *J. Am. Chem. Soc*, 1986, 108, 7228-7230.
14. Alain Roucoux, Jurgen Schulz, Henri Patin ,*Chem.Rev*, 2002, 102, 3757-3778.
15. A. Biffis, N.orlandi, B. Corain, *Adv.Mater*, 2003, 15, 1551.
16. Sakai T, Alexandridis P, *Langmuir*, 2004, 20, 8426.
17. Mandal S, Rao VG, Ghosh S, Sarkar N *J Phys.Chem. C* 2012, 116, 5586.
18. Robert W.J Scott , Richard M Crooks, *J Phys. Chem. B*, 2005, 109, 692.
19. C. Wang, N.T.Flynn, R. Langer, , *Adv. Mater.*, 2004, 16, 1074.
20. X. Ding, X. Zhao, Z. Deng, X.Zengh,Z. Y. Peng, X. Long, , *Macromol. Rapid Commun.* , 2005, 26, 1784.
21. Palapparambil Sunny Gils , Debajyoti Ray, Prafulla Kumar Sahooa, *Int J Biol Macromol*, 2010, 46, 237-244.
22. Masayuki Tomida, Takeshi Nakato, *Polymer*, 1997, 38, 4733-4736.
23. Manuela T. Nistor, Aurica P, Loredana E. Nita, Iordana Neamtu, Cornelia Vasile, *Polymer Engineering and science*, 2013, 1-8.
24. Yiyang Lin, Yan Qiao, Yijie Wang, Yun Yan and Jianbin Huang, *J. Mater. Chem.*, 2012, 22, 18314-18320.

25. Y. Murali Mohan , Varsha Thomas , K. Varaprasad , B. Sreedhar , S.K. Bajpai ,K. Mohana Raju, *Journal of Colloid and Interface Science* 2010, 342, 73-82.

26. Palapparambil Sunny Gils , Debajyoti Ray, Prafulla Kumar Sahooa, *Int J Biol Macromol*, 2010, 46, 237-244.

27. Y. Murali Mohan, Kyungjae Lee, Thathan Premkumar, Kurt E. Geckeler, *Polymer*, 2007, 48, 158-164.

28. Pangkita Deka, Ramesh C. Dekha, Pankaj Bharali, *New J. Chem.*, 2014, 38, 1789-1793.

Graphical Abstract